JOURNAL OF MODERN OPTICS, 2018
VOL. 65, NO. 12, 1437–1441
https://doi.org/10.1080/09500340.2018.1443223

Taylor & Francis
Taylor & Francis Group

Polarization and coherence in the Hanbury Brown–Twiss effect

Xianlong Liu[a,b], Gaofeng Wu[c], Xiaoyan Pang[d], David Kuebel[e,f] and Taco D. Visser[d,f,g]

[a]College of Physics, Optoelectronics and Energy & Collaborative, Innovation, Center of Suzhou Nano Science and Technology, Soochow University, Suzhou, China; [b]Key Lab of Advanced Optical Manufacturing Technologies of Jiangsu Province & Key Lab of Modern Optical Technologies of Education Ministry of China, Soochow University, Suzhou, China; [c]School of Physics, Northwest University, Xi'an, China; [d]School of Electronics and Information, Northwestern Polytechnical University, Xi'an, China; [e]St. John Fisher College, Rochester, NY, USA; [f]Department of Physics and Astronomy, University of Rochester, Rochester, NY, USA; [g]Department of Physics and Astronomy, Vrije Universiteit, Amsterdam, The Netherlands

ABSTRACT

We study the correlation of intensity fluctuations in random electromagnetic beams, the so-called Hanbury Brown–Twiss effect (HBT). We show that not just the state of coherence of the source, but also its state of polarization has a strong influence on the far-zone correlations. Different types of sources are found to have different upper bounds for the normalized HBT coefficient.

ARTICLE HISTORY
Received 31 October 2017
Accepted 12 February 2018

KEYWORDS
Coherence; electromagnetic optics; polarization; random beams; Hanbury Brown–Twiss effect

1. Introduction

In their landmark experiment, Hanbury Brown and Twiss studied the correlation of intensity fluctuations at two detectors with a variable separation distance, to determine the angular diameter of radio stars (*1*–*3*). Since then the eponymous Hanbury Brown–Twiss effect (HBT) has been applied in many other fields, such as nuclear physics (*4*) and atomic physics (*5*–*7*). In optics, it has been used to study certain inverse problems (*8*, *9*), and to determine the mode index of vortex beams (*10*). It is also explored in classical versions of ghost imaging (*11*).

In the original astronomical studies that were carried out by Hanbury Brown and Twiss, polarization issues could be ignored, and therefore a scalar description sufficed (*12*, Ch. 7). A generalization to random electromagnetic beams, as generated for example, by multi-mode lasers, can be found in (*13*, Ch. 8). In recent years, several studies were dedicated to the correlation of intensity fluctuations in such beams, among them (*14*, *15*), in which the degree of cross-polarization was introduced. The usefulness of this concept has been questioned in (*16*). The evolution of the HBT effect during propagation was studied in (*17*, *18*).

In the present study, we examine the far-zone HBT effect that occurs in a wide class of partially coherent beams, the so-called Electromagnetic Gaussian Schell-Model (EGSM) beams (*12*). As we will demonstrate, not just the state of coherence of the source, but also its state of polarization plays a major role. Also, different types of sources are found to have different upper bounds for the normalized HBT coefficient.

2. The HBT effect in random electromagnetic beams

We consider a stochastic, wide-sense stationary, electromagnetic beam propagating close to the z axis into the half-space $z > 0$ (see Figure 1). The vector $\boldsymbol{\rho} = (x, y)$ denotes a transverse position. To simplify the notation, we will from here on suppress the ω dependence of the various quantities. In the space–frequency formulation of coherence theory, the coherence and polarization properties of a beam at two points $\boldsymbol{\rho}_1$ and $\boldsymbol{\rho}_2$ in the same transverse plane z can be described by its cross-spectral density (CSD) matrix (*12*)

$$\mathbf{W}(\boldsymbol{\rho}_1, \boldsymbol{\rho}_2, z) = \begin{pmatrix} W_{xx}(\boldsymbol{\rho}_1, \boldsymbol{\rho}_2, z) & W_{xy}(\boldsymbol{\rho}_1, \boldsymbol{\rho}_2, z) \\ W_{yx}(\boldsymbol{\rho}_1, \boldsymbol{\rho}_2, z) & W_{yy}(\boldsymbol{\rho}_1, \boldsymbol{\rho}_2, z) \end{pmatrix}, \quad (1)$$

with

$$W_{ij}(\boldsymbol{\rho}_1, \boldsymbol{\rho}_2, z) = \langle E_i^*(\boldsymbol{\rho}_1, z) E_j(\boldsymbol{\rho}_2, z) \rangle, \quad (i, j = x, y), \quad (2)$$

where the angled brackets denote an ensemble average. The intensity of a single realization of the beam is defined as

CONTACT Taco D. Visser tvisser@nat.vu.nl

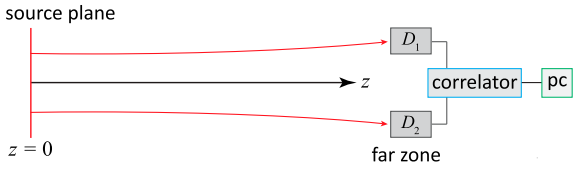

Figure 1. Illustrating the Hanbury Brown–Twiss experiment. D_1 and D_2 are intensity detectors, located in the far zone at $(\boldsymbol{\rho}_1, z)$ and $(\boldsymbol{\rho}_2, z)$, whose output is sent to a correlator that is connected to a pc.

$$I(\boldsymbol{\rho}, z) = |E_x(\boldsymbol{\rho}, z)|^2 + |E_y(\boldsymbol{\rho}, z)|^2, \tag{3}$$

whereas its expectation value

$$\langle I(\boldsymbol{\rho}, z)\rangle = \langle |E_x(\boldsymbol{\rho}, z)|^2\rangle + \langle |E_y(\boldsymbol{\rho}, z)|^2\rangle \tag{4}$$

$$= \mathrm{Tr}\, \mathbf{W}(\boldsymbol{\rho}, \boldsymbol{\rho}, z), \tag{5}$$

where Tr denotes the trace. The intensity variation is given by the expression

$$\Delta I(\boldsymbol{\rho}, z) = I(\boldsymbol{\rho}, z) - \langle I(\boldsymbol{\rho}, z)\rangle. \tag{6}$$

We can introduce a measure of the correlation of intensity fluctuations at two points by defining the HBT coefficient as

$$C(\boldsymbol{\rho}_1, \boldsymbol{\rho}_2, z) = \langle \Delta I(\boldsymbol{\rho}_1, z) \Delta I(\boldsymbol{\rho}_2, z)\rangle. \tag{7}$$

If the source fluctuations are governed by Gaussian statistics, one can use the Gaussian moment theorem to derive that (*14*, Equation (8))

$$C(\boldsymbol{\rho}_1, \boldsymbol{\rho}_2, z) = \sum_{i,j} \left| W_{ij}(\boldsymbol{\rho}_1, \boldsymbol{\rho}_2, z)\right|^2. \tag{8}$$

It is convenient to use a normalized correlation coefficient, indicated by the subscript N, namely

$$C_N(\boldsymbol{\rho}_1, \boldsymbol{\rho}_2, z) = \frac{C_0(\boldsymbol{\rho}_1, \boldsymbol{\rho}_2, z)}{\langle I(\boldsymbol{\rho}_1, z)\rangle \langle I(\boldsymbol{\rho}_2, z)\rangle} \tag{9}$$

$$= \frac{\sum_{i,j} \left| W_{ij}(\boldsymbol{\rho}_1, \boldsymbol{\rho}_2, z)\right|^2}{\mathrm{Tr}\, \mathbf{W}(\boldsymbol{\rho}_1, \boldsymbol{\rho}_1, z)\, \mathrm{Tr}\, \mathbf{W}(\boldsymbol{\rho}_2, \boldsymbol{\rho}_2, z)}. \tag{10}$$

It can be shown (*16*) that $0 \le C_N(\boldsymbol{\rho}_1, \boldsymbol{\rho}_2, z) \le 1$.

3. Electromagnetic Gaussian Schell-model beams

The cross-spectral density matrix elements of an EGSM beam in the source plane $z = 0$ read

$$W_{ij}(\boldsymbol{\rho}_1, \boldsymbol{\rho}_2, 0)$$

$$= A_i A_j B_{ij} \exp\left[-\frac{\boldsymbol{\rho}_1^2}{4\sigma_i^2} - \frac{\boldsymbol{\rho}_2^2}{4\sigma_j^2} - \frac{(\boldsymbol{\rho}_1 - \boldsymbol{\rho}_2)^2}{2\delta_{ij}^2}\right]. \tag{11}$$

The source parameters A_i, B_{ij}, σ_i and δ_{ij} are independent of position, but may depend on frequency. For their physical meaning, we refer to (*19*, *20*). We will restrict ourselves to the case where the width of the spectral densities associated with E_x and E_y are equal, i.e. we assume that $\sigma_x = \sigma_y = \sigma$. The parameters have to satisfy several constraints, i.e. (*12*, Sec. 9.4.2)

$$B_{xx} = B_{yy} = 1, \tag{12}$$

$$B_{xy} = B_{yx}^*, \tag{13}$$

$$\left|B_{xy}\right| \le 1, \tag{14}$$

$$\delta_{xy} = \delta_{yx}. \tag{15}$$

Furthermore, the two conditions for the source to generate a beam-like field are (*21*)

$$\frac{1}{4\sigma^2} + \frac{1}{2\delta_{ii}^2} \ll \frac{2\pi^2}{\lambda^2}. \tag{16}$$

And finally, the non-negativeness of the cross-spectral density matrix implies that (*22*)

$$\sqrt{\frac{\delta_{xx}^2 + \delta_{yy}^2}{2}} \le \delta_{xy} \le \sqrt{\frac{\delta_{xx}\delta_{yy}}{|B_{xy}|}}. \tag{17}$$

After propagating a distance z through free space, the CSD matrix elements evolve into (see (*12*), where the one but last minus sign in Equation (10) on p. 184 should be a plus sign):

$$W_{ij}(\boldsymbol{\rho}_1, \boldsymbol{\rho}_2, z) = \frac{A_i A_j B_{ij}}{\Delta_{ij}^2(z)} \exp\left[-\frac{(\boldsymbol{\rho}_1 + \boldsymbol{\rho}_2)^2}{8\sigma^2 \Delta_{ij}^2(z)}\right] \times \exp\left[-\frac{(\boldsymbol{\rho}_1 - \boldsymbol{\rho}_2)^2}{2\Omega_{ij}^2 \Delta_{ij}^2(z)} + \frac{ik(\rho_2^2 - \rho_1^2)}{2R_{ij}(z)}\right], \tag{18}$$

where

$$\frac{1}{\Omega_{ij}^2} = \frac{1}{4\sigma^2} + \frac{1}{\delta_{ij}^2}, \tag{19}$$

$$\Delta_{ij}^2(z) = 1 + (z/\sigma k \Omega_{ij})^2, \tag{20}$$

$$R_{ij}(z) = [1 + (\sigma k \Omega_{ij}/z)^2]z, \tag{21}$$

and $k = \omega/c$ is the wavenumber, c being the speed of light. Because we intend to study the HBT effect in the far zone of the source, we note for future use that

$$\lim_{z\to\infty}\Delta_{ij}^2(z)=\frac{z^2}{(\sigma k\Omega_{ij})^2}, \tag{22}$$

$$\lim_{z\to\infty}R_{ij}(z)=z. \tag{23}$$

We will apply Equations (18), (22) and (23) to beams that are generated by different types of sources.

4. Unpolarized beams

For a rotationally symmetric, unpolarized source that generates an EGSM beam, we have that

$$A_x=A_y=A, \tag{24}$$

$$\delta_{xx}=\delta_{yy}=\delta, \tag{25}$$

$$B_{xy}=B_{yx}=0, \tag{26}$$

$$\delta_{xy}=\delta_{yx}=0. \tag{27}$$

The two non-zero matrix elements are equal, i.e.

$$W_{xx}(\boldsymbol{\rho}_1,\boldsymbol{\rho}_2,z)=W_{yy}(\boldsymbol{\rho}_1,\boldsymbol{\rho}_2,z)=W(\boldsymbol{\rho}_1,\boldsymbol{\rho}_2,z), \tag{28}$$

with, in the far zone,

$$W(\boldsymbol{\rho}_1,\boldsymbol{\rho}_2,z)=\left(\frac{Ak\sigma\Omega}{z}\right)^2\exp\left[-\frac{(\boldsymbol{\rho}_1+\boldsymbol{\rho}_2)^2k^2\Omega^2}{8z^2}\right]\times\exp\left[-\frac{(\boldsymbol{\rho}_2-\boldsymbol{\rho}_1)^2k^2\sigma^2}{2z^2}\right]\times\exp\left(\mathrm{i}k\frac{\rho_2^2-\rho_1^2}{2z}\right), \tag{29}$$

where

$$\frac{1}{\Omega^2}=\frac{1}{4\sigma^2}+\frac{1}{\delta^2}. \tag{30}$$

If we take the first reference point to be on the z axis ($\boldsymbol{\rho}_1=\mathbf{0}$), then it is seen from Equation (29) that $W(\mathbf{0},\boldsymbol{\rho}_2,z)$ is rotationally symmetric, i.e. it depends only on $\rho_2=|\boldsymbol{\rho}_2|$. In the far-field, the polar angle $\theta\approx\tan\theta=\rho_2/z$. Hence, the matrix elements can be expressed as

$$W(\mathbf{0},\theta,z)=\left(\frac{Ak\sigma\Omega}{z}\right)^2\exp\left(-\frac{\theta^2k^2\Omega^2}{8}\right)\times\exp\left(-\frac{\theta^2k^2\sigma^2}{2}\right)\exp\left(\mathrm{i}k\frac{\theta^2z}{2}\right). \tag{31}$$

Using Equation (8), we obtain for the HBT coefficient the formula

$$C(\mathbf{0},\theta,z)=2\left(\frac{Ak\sigma\Omega}{z}\right)^4\exp\left(-\frac{\theta^2k^2\Omega^2}{4}\right)\times\exp\left(-\theta^2k^2\sigma^2\right). \tag{32}$$

From Equations (32) and (10), one readily finds that the normalized HBT coefficent is given by the expression

$$C_N(\mathbf{0},\theta)=\frac{1}{2}\exp\left(-\frac{\theta^2k^2\Omega^2}{4}\right)\exp\left(-\theta^2k^2\sigma^2\right) \tag{33}$$

$$=\frac{1}{2}\exp\left(-\frac{4\theta^2k^2\sigma^4}{\delta^2+4\sigma^2}\right), \tag{34}$$

where the z dependence has dropped out. It is evident from Equation (34) that the far-zone HBT coefficient of an unpolarized, rotationally symmetric beam depends on both the effective source size σ and the correlation length δ. Also, it is seen that this coefficient has an upper bound of 1/2.

5. Linearly polarized beams

Let us next consider a source that is linearly polarized along the x direction. We then have

$$A_x=A, \tag{35}$$

$$\delta_{xx}=\delta. \tag{36}$$

The only non-zero matrix element, $W_{xx}(\boldsymbol{\rho}_1,\boldsymbol{\rho}_2,z)$, takes on the far-zone form

$$W_{xx}(\boldsymbol{\rho}_1,\boldsymbol{\rho}_2,z)=\left(\frac{Ak\sigma\Omega}{z}\right)^2\exp\left[-\frac{(\boldsymbol{\rho}_1+\boldsymbol{\rho}_2)^2k^2\Omega^2}{8z^2}\right]\times\exp\left[-\frac{(\boldsymbol{\rho}_2-\boldsymbol{\rho}_1)^2k^2\sigma^2}{2z^2}\right]\times\exp\left(\mathrm{i}k\frac{\rho_2^2-\rho_1^2}{2z}\right). \tag{37}$$

As before, we take the first reference point, $\boldsymbol{\rho}_1$, to be on the z axis. Again expressing the relevant quantities in terms of the polar angle θ, we obtain for the HBT coefficient the expression

$$C(\mathbf{0},\theta,z)=\left(\frac{Ak\sigma\Omega}{z}\right)^4\exp\left(-\frac{\theta^2k^2\Omega^2}{4}\right)\times\exp\left(-\theta^2k^2\sigma^2\right). \tag{38}$$

Hence, its normalized version

$$C_N(\mathbf{0},\theta)=\exp\left(-\frac{4\theta^2k^2\sigma^4}{\delta^2+4\sigma^2}\right). \tag{39}$$

It is seen that the far-zone HBT coefficient for a linearly polarized EGSM beam does not depend on the direction of polarization. Furthermore, it is twice as large as the coefficient for unpolarized light, as given by Equation (34), the upper bound now being unity.

6. Partially polarized beams

As a third example, we study a partially polarized, rotationally symmetric source. In that case,

$$A_x = A_y = A, \tag{40}$$
$$\delta_{xx} = \delta_{yy} = \delta. \tag{41}$$

It immediately follows that

$$\Omega_{xx} = \Omega_{yy} = \Omega \neq \Omega_{xy}, \tag{42}$$
$$\Delta_{xx} = \Delta_{yy} = \Delta \neq \Delta_{xy}. \tag{43}$$

The two inequalities follow from the fact that, in general, $\delta_{xy} \neq \delta$. For the four matrix elements, we now have the far-zone formulas

$$\begin{aligned} W_{xx}(\boldsymbol{\rho}_1, \boldsymbol{\rho}_2, z) &= W_{yy}(\boldsymbol{\rho}_1, \boldsymbol{\rho}_2, z) \qquad (44)\\ &= \left(\frac{Ak\sigma\Omega}{z}\right)^2 \exp\left[-\frac{(\boldsymbol{\rho}_1+\boldsymbol{\rho}_2)^2 k^2\Omega^2}{8z^2}\right] \\ &\quad \times \exp\left[-\frac{(\boldsymbol{\rho}_2-\boldsymbol{\rho}_1)^2 k^2\sigma^2}{2z^2}\right] \\ &\quad \times \exp\left(\mathrm{i}k\frac{\rho_2^2-\rho_1^2}{2z}\right), \qquad (45)\\ W_{xy}(\boldsymbol{\rho}_1, \boldsymbol{\rho}_2, z) &= B_{xy}\left(\frac{Ak\sigma\Omega_{xy}}{z}\right)^2 \\ &\quad \times \exp\left[-\frac{(\boldsymbol{\rho}_1+\boldsymbol{\rho}_2)^2 k^2\Omega_{xy}^2}{8z^2}\right] \\ &\quad \times \exp\left[-\frac{(\boldsymbol{\rho}_2-\boldsymbol{\rho}_1)^2 k^2\sigma^2}{2z^2}\right] \\ &\quad \times \exp\left(\mathrm{i}k\frac{\rho_2^2-\rho_1^2}{2z}\right), \qquad (46)\\ W_{yx}(\boldsymbol{\rho}_1, \boldsymbol{\rho}_2, z) &= B_{xy}^*\left(\frac{Ak\sigma\Omega_{xy}}{z}\right)^2 \\ &\quad \times \exp\left[-\frac{(\boldsymbol{\rho}_1+\boldsymbol{\rho}_2)^2 k^2\Omega_{xy}^2}{8z^2}\right] \\ &\quad \times \exp\left[-\frac{(\boldsymbol{\rho}_2-\boldsymbol{\rho}_1)^2 k^2\sigma^2}{2z^2}\right] \\ &\quad \times \exp\left(\mathrm{i}k\frac{\rho_2^2-\rho_1^2}{2z}\right), \qquad (47) \end{aligned}$$

where in the last expression we made use of the fact that $B_{yx} = B_{xy}^*$ and $\Omega_{yx} = \Omega_{xy}$. Taking the first reference point $\boldsymbol{\rho}_1$ on axis and expressing the relevant quantities in terms of the angle θ, we thus find for the HBT coefficient the formula

$$\begin{aligned} C(\mathbf{0}, \theta, z) &= 2\left(\frac{Ak\sigma}{z}\right)^4 \exp\left(-\theta^2 k^2\sigma^2\right) \\ &\quad \times \left[\Omega^4 \exp\left(-\frac{\theta^2 k^2\Omega^2}{4}\right)\right. \\ &\quad \left. + |B_{xy}|^2\Omega_{xy}^4 \exp\left(-\frac{\theta^2 k^2\Omega_{xy}^2}{4}\right)\right]. \qquad (48) \end{aligned}$$

A straightforward calculation then yields the equations

$$\begin{aligned} C_N(\mathbf{0}, \theta) &= \frac{1}{2}\exp\left[-\theta^2 k^2\left(\sigma^2 - \frac{\Omega^2}{2}\right)\right] \\ &\quad \times \left\{\exp\left[-\left(\frac{\theta k\Omega}{2}\right)^2\right]\right. \\ &\quad \left. + \left(\frac{\Omega_{xy}}{\Omega}\right)^4 |B_{xy}|^2 \exp\left[-\left(\frac{\theta k\Omega_{xy}}{2}\right)^2\right]\right\} \qquad (49)\\ &= \frac{1}{2}\exp\left(-\frac{4\theta^2 k^2\sigma^4}{\delta^2+4\sigma^2}\right) \\ &\quad \times \left\{1 + |B_{xy}|^2\left(\frac{\Omega_{xy}}{\Omega}\right)^4\right. \\ &\quad \left. \times \exp\left[-\frac{\theta^2 k^2(\Omega_{xy}^2-\Omega^2)}{4}\right]\right\}. \qquad (50) \end{aligned}$$

Equation (50) shows that the normalized far-zone HBT coefficient of a rotationally symmetric, partially polarized source depends on its effective size σ, the two coherence lengths δ and δ_{xy}, and the parameter B_{xy}. Compared to the unpolarized case, given by Equation (34), the coefficient is now larger, due to the presence of the factor between curly brackets that is always greater than unity. The upper bound now exceeds 1/2 due to the fact that $|B_{xy}| > 0$ for partially polarized sources. Clearly, a non-zero correlation between the two Cartesian components of the electric field in the source plane increases the correlation of the intensity fluctuations in the far zone. It is worth pointing out that the constraint expressed by (17) defines an upper limit for the value of $|B_{xy}|$.

We illustrate our results in Figure 2 in which the far-zone normalized HBT coefficient is plotted for three different kinds of EGSM sources, i.e. an unpolarized source, a linearly polarized source and a partially polarized source. The coefficient for the linearly polarized case is the only one with a unit upper bound, and its value always exceeds that of the other cases. The partially coherent source produces an HBT coefficent that, at all observation angles, is larger than that of its unpolarized counterpart.

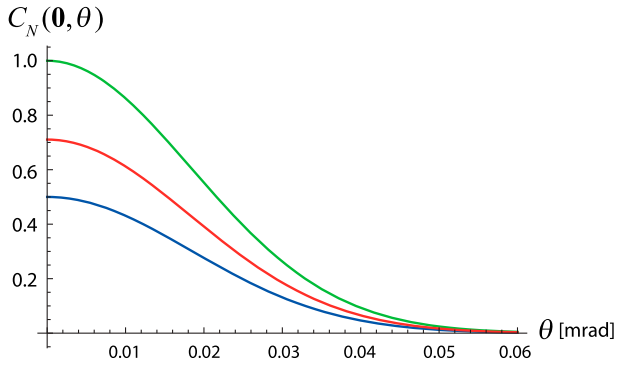

Figure 2. The normalized far-zone Hanbury Brown–Twiss coefficient for three EGSM sources with different states of polarization: linearly polarized (green curve), partially polarized (red curve) and unpolarized (blue curve). In these examples, the parameters are: $\lambda = 632.8$ nm, $\sigma = 4$ mm, $\delta = 2$ mm, $\delta_{xy} = 2.3$ mm and $B_{xy} = 0.5$.

7. Conclusions

We have examined the Hanbury Brown–Twiss effect that occurs in random beams generated by electromagnetic Gaussian Schell-model sources. Expressions for the normalized far-zone HBT coefficient were derived in terms of the source parameters. This coefficient was shown to have an upper limit that depends on the state of coherence and polarization in the source plane. Our results show that the far-zone HBT effect coefficient can be used to obtain properties of the source.

Disclosure statement

No potential conflict of interest was reported by the authors.

Funding

This material is based upon work supported by the Air Force Office of Scientific Research [award number FA9550-16-1-0119]. GW acknowledges support from the Natural Science Basic Research Plan of Shaanxi Province of China [grant number 2016JQ1021]. XL is supported by the China Scholarship Council (CSC) [grant number 201606920060]. This work is partly supported by the National Natural Sciences Foundation of China (NSFC) [grant number 11504296]; and the Natural Science Basic Research Plan in Shaanxi Province of China [program number 2016JQ1011].

References

(1) Hanbury Brown, R.; Twiss, R.Q. A New Type of Interferometer for Use in Radio Astronomy. *Phil. Magazine* **1954,** *45,* 663–682.
(2) Hanbury Brown, R.; Twiss, R.Q. Correlation between Photons in Two Coherent Beams of Light. *Nature* **1956,** *177,* 27–29.
(3) Hanbury Brown, R. *The Intensity Interferometer*; Taylor and Francis, London, 1974.
(4) Baym, G. The Physics of Hanbury Brown-Twiss Intensity Interferometry: From Stars to Nuclear Collisions. *Acta Phys. Pol. B* **1998,** *29,* 1839–1884.
(5) Öttl, A.; Ritter, S.; Köhl, M.; Esslinger, T. Correlations and Counting Statistics of an Atom Laser. *Phys. Rev. Lett.* **2005,** *95,* 090404.
(6) Schellekens, M.; Hoppeler, R.; Perrin, A. Viana Gomes, J.; Boiron, D.; Aspect, A.; Westbrook, C.I. Hanbury Brown-Twiss Effect for Ultracold Quantum Gases. *Science* **2005,** *310,* 648–651.
(7) Jeltes, T.; McNamara, J.M.; Hogervorst, W.; Vassen, W.; Krachmalnicoff, V.; Schellekens, M.; Perrin, A.; Chang, H.; Boiron, D.; Aspect, A.; Westbrook, C.I. Comparison of the Hanbury Brown-Twiss Effect for Bosons and Fermions. *Nature* **2007,** *445,* 402–405.
(8) Kuebel, D.; Visser, T.D.; Wolf, E. Application of the Hanbury Brown-Twiss Effect to Scattering from Quasi-homogeneous Media. *Opt. Commun.* **2013,** *294,* 43–48.
(9) Wu, G.; Visser, T.D. Correlation of Intensity Fluctuations in Beams Generated by Quasi-homogeneous Sources. *J. Opt. Soc. Am. A* **2014,** *31,* 2152–2159.
(10) Liu, R.; Wang, F.; Chen, D.; Wang, Y.; Zhou, Y.; Gao, H.; Zhang, P.; Li, F. Measuring Mode Indices of a Partially Coherent Vortex Beam with Hanbury Brown and Twiss Type Experiment. *Appl. Phys. Lett.* **2016,** *108,* 051107.
(11) Shirai, T. Modern Aspects of Intensity Interferometry with Classical Light. In *Progress in Optics*Vol. 62,; Visser, T.D., Ed.; Elsevier, Amsterdam, 2017; pp 1–72.
(12) Wolf, E. *Introduction to the Theory of Coherence and Polarization of Light*; Cambridge University Press, Cambridge, 2007.
(13) Mandel, L.; Wolf, E. *Optical Coherence and Quantum Optics*; Cambridge University Press, Cambridge, 1995.
(14) Shirai, T.; Wolf, E. Correlations between Intensity Fluctuations in Stochastic Electromagnetic Beams of Any State of Coherence and Polarization. *Opt. Commun.* **2007,** *272,* 289–292.
(15) Al-Qasimi, A.; Lahiri, M.; Kuebel, D.; James, D.F.V.; Wolf, E. The Influence of the Degree of Cross-polarization on the Hanbury Brown-Twiss Effect. *Opt. Express* **2010,** *18,* 17124–17129.
(16) Hassinen, T.; Tervo, J.; Setälä, T.; Friberg, A.T. Hanbury Brown-Twiss Effect with Electromagnetic Waves. *Opt. Express* **2011,** *19,* 15188–15195.
(17) Li, Y. Correlations between Intensity Fluctuations in Stochastic Electromagnetic Gaussian Schell-model Beams. *Opt. Commun.* **2014,** *316,* 67–73.
(18) Wu, G.; Visser, T.D. Hanbury Brown-Twiss Effect with Partially Coherent Electromagnetic Beams. *Opt. Lett.* **2014,** *39,* 2561–2564.
(19) Gori, F.; Santarsiero, M.; Piquero, G.; Borghi, R.; Mondello, A.; Simon, R. Partially Polarized Gaussian Schell-model Beams. *J. Opt. A* **2001,** *3,* 1–9.
(20) Wolf, E. Unified Theory of Coherence and Polarization of Random Electromagnetic Beams. *Phys. Lett. A* **2003,** *312,* 263–267.
(21) Korotkova, O.; Salem, M.; Wolf, E. Beam Conditions for Radiation Generated by an Electromagnetic Gaussian Schell-model Source. *Opt. Lett.* **2004,** *29,* 1173–1175.
(22) Gori, F.; Santarsiero, M.; Borghi, R.; Ramírez-Sánchez, V. Realizability Condition for Electromagnetic Schell-model Sources. *J. Opt. Soc. Am. A* **2008,** *25,* 1016–1021.